RSC Advances

PAPER

View Article Online
View Journal | View Issue

Cite this: *RSC Adv.*, 2024, **14**, 34925

A rapid and scalable method for visible light induced bromination of uracil derivatives in a falling film looping photoreactor†

Shibu Naskar,‡ Susital Mal,‡ Shivangi Shivangi and Subrata Das *

Visible light induced green synthesis of 5-bromouracil derivatives using *N*-bromosuccinimide (NBS) in acetonitrile under batch operation with a constant photon flux of 46 μmol s^{-1} is reported. This methodology has shown excellent tolerance with various 6-substituted and *N*-substituted uracils and is also applicable for various pyrimidine and arene derivatives. The reaction proceeded through the formation of a bromine molecule *via* a radical pathway followed by an electrophilic substitution reaction, and this hybrid nature of the reaction pathway in the presence of light made the process faster. We successfully synthesized twenty-one derivatives and characterized them using various spectroscopic methods. Finally, the three different modules of the looping falling film reactor were used to show the successive scalability of the process with comparable photonic characteristics and reaction conditions. We achieved milligram to multigram scale reaction with almost equal efficiency and maximum productivity up to 1.2 kg per day.

Received 9th August 2024
Accepted 22nd October 2024

DOI: 10.1039/d4ra05774k

rsc.li/rsc-advances

Introduction

Uracil and its derivatives are among the most abundant moieties frequently found in biologically active molecules and pharmaceuticals.[1–6] Radioactive halogenated uracil nucleoside probes are used to study DNA metabolism.[7] Many biologically active nucleoside analogs are also prepared from halogenated nucleosides (Chart 1).[8–13] Moreover, it has been shown that for the synthesis of flavins known as organophotocatalysts and thymidine phosphorylase inhibitors, 6-chloro-5-bromouracil is used as a key intermediate.[14,15] Hence, developing a new methodology for the synthesis of 5-halouracil derivatives by using mild and effective scalable conditions has always been appreciated in medicinal and other branches of chemistry.

Several reagents like $CuBr_2$,[16] NaBr,[17] 1-butyl-pyridinium bromide[18] and tetrabutylammonium tribromide[19] have already been reported for bromination at sp^2-carbon in the presence of strong oxidizing agents such as $K_2S_2O_8$, H_2O_2 and oxone. The main disadvantage of the above-reported methods is that they promote toxic reagents and oxidants, resulting in environmental pollution. Chen *et al.* reported an electrochemical method for the *meta*-selective bromination of pyridine.[20] However, this method has not yet been tested with uracil derivatives, and a 10 mmol reaction needs 38 hours, indicating that the reaction is prolonged. Thus, scalability is an issue with low yield (69%). Molecular bromine has widely been used for the bromination of uracil derivatives.[21–24] However, molecular bromine is very toxic; sometimes, it is used with hazardous solvents like CCl_4 and strong chemical oxidants like peroxide. *N*-Bromosuccinimide (NBS) is another widely known brominating agent and has also been reported to be used for the bromination of uracil derivatives.[25,26] Although NBS is a relatively safer reagent than molecular bromine, bromination applying NBS in refluxing CCl_4 in the presence of a radical initiator like peroxide is not a good choice.[27] This is because CCl_4 is a toxic and ozone-depleting solvent[28,29] and it is internationally banned by Montreal Protocol[30] and thus prohibited for industrial use. The rapid development in radical chemistry promoted several innovative strategies for organic and materials chemistry.[31–34] The visible or UV light-induced benzylic bromination[35–40] and bromination of arenes have also been reported as a green energy process.[41,42] The light-induced strategies are one of the most selective, economical, greenest, and safest one.[43–46] However, they also have limitations regarding scalability concerns. This is because most photochemical reactions depend on the absorption of photons in stoichiometric quantities. Beer–Lambert law describes the photophysical conditions like the exponential decay of the photon flux with the depth of the reaction vessel, which limits the availability of photons for a reagent in any photochemical reaction. Trifluoromethylation of *N*-Boc-pyrrole reported by Beatty and co-workers showed that the simple scaling of the lab-

Department of Chemistry, National Institute of Technology Patna, Bihar 800005, India. E-mail: subratad@nitp.ac.in

† Electronic supplementary information (ESI) available: General information, characterization data, experimental procedures, ^1H & ^{13}C-NMR spectra. CCDC 2329775, 2348542 and 2380150. For ESI and crystallographic data in CIF or other electronic format see DOI: https://doi.org/10.1039/d4ra05774k

‡ These authors contributed equally.

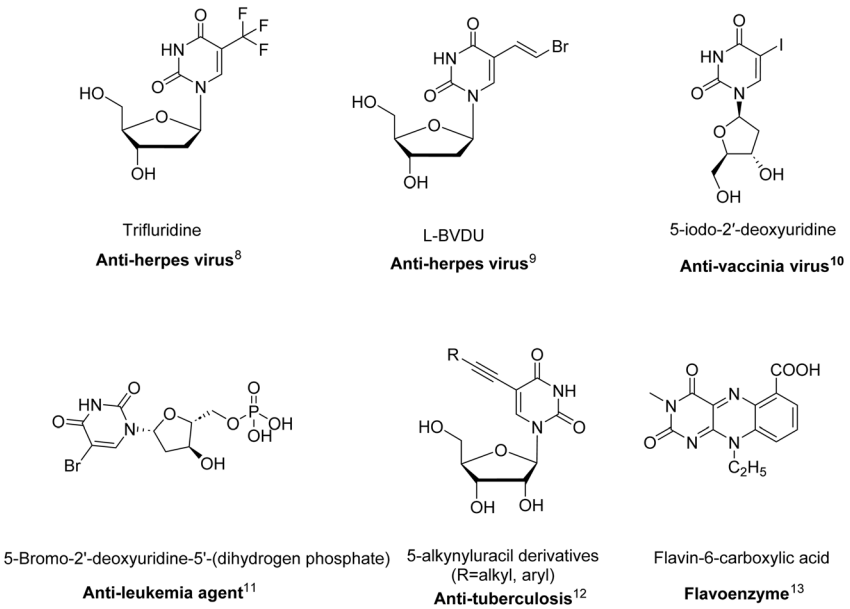

Chart 1 Representative pharmaceuticals containing 5-halouracil as an intermediated.

based batch reaction from 18.3 g to 100 g reduced the yield significantly by around 39% with a significant increase in reaction time from 15 h to 62 h by using the same batch condition and the same light source.[47] This proves the importance of relative photon availability per substrate molecule for a photochemical reaction. Cantillo and co-workers[48] demonstrated visible light induced scalable benzylic bromination by using NBS in continuous flow. Recently, the scale-up strategy for the same reaction was shown using a looping falling film reactor developed by our group.[49] The falling film looping photoreactor allows small-scale photoreactions to be carried out on a laboratory scale. It demonstrates the scalability of the reactor concept without major changes to the reaction conditions by counteracting light attenuation, counteracting heat transfer, counteracting mass transport limitation, and ensuring comparable optical characteristics along the different scales of the photoreactors. This reactor can also carry out batch operations with specific photon flux without applying a looping film. This method of visible light-mediated bromination for uracil derivatives using NBS has not been reported to date (Scheme 1). So, if we can achieve this with scalability, this might contribute some value to the scientific community as a safer, greener, faster and scalable protocol for bromination of uracil derivatives.

In this article, we used a falling film looping photoreactor to develop a new methodology and rapid scale-up strategy of visible light induced bromination reaction of uracil derivatives in the presence of NBS in acetonitrile. Simple batch operations were performed on a lab scale with 46 μmol s^{-1} photon flux at 25–30 °C just to show the feasibility and derivative scope of the reaction. After the successful laboratory experiment, a falling film looping-batch operation was performed to show the successive scalability of this reaction protocol with comparable optical characteristics and conditions. It was found that with the falling film looping operation, every scale-up reaction was completed within 15 minutes with maximum productivity of up to 1.2 kg per day. An initial version of this work was deposited in ChemRxiv on 11.12.2023.[50]

Result and discussion

The optimization process started with determining the exact amount of NBS required for the reaction. For this, 1 equivalent of 6-chloro-3-methyluracil (**1**) and 1.05 equivalent NBS were dissolved in 1 mL of acetonitrile under 21 μmol s^{-1} constant photon flux in falling film looping photoreactor without looping operation. Product **1a** was formed with a 48% yield, and the starting material was not completely consumed after 10 hours (entry 1, Table 1). The same procedure was repeated using 1.3, 1.5, 1.8, 2, and 2.2 equivalents of NBS separately (entries 2–6, Table 1). To our surprise, it was found that with 2.2 equivalent of NBS, starting material was fully consumed within 5 hours with an 84% yield. This is quite surprising because the amount of NBS required was almost double that of the previously reported method (Scheme 1). This might be due to the formation of molecular bromine *via* the free radical pathway, which helped to propagate the reaction. For this reason, the reaction solution turned deep red during the reaction (Fig. S13†).

The optimum photon flux was determined after determining the amount of NBS required for the reaction. We have commenced our investigation by performing the reaction separately in 21 μmol s^{-1}, 38 μmol s^{-1} and 46 μmol s^{-1} constant photon flux within 1XA irradiation module. It was found that increasing the photon flux gradually from 21 μmol s^{-1} to 46 μmol s^{-1}, reducing the reaction time from 5 hours to 1 hour, respectively (entries 1–3, Table 2). Interestingly, the reaction time dropped to 20 minutes when we raised the photon flux further (~92 μmol s-1), although the yield also dropped to 79%

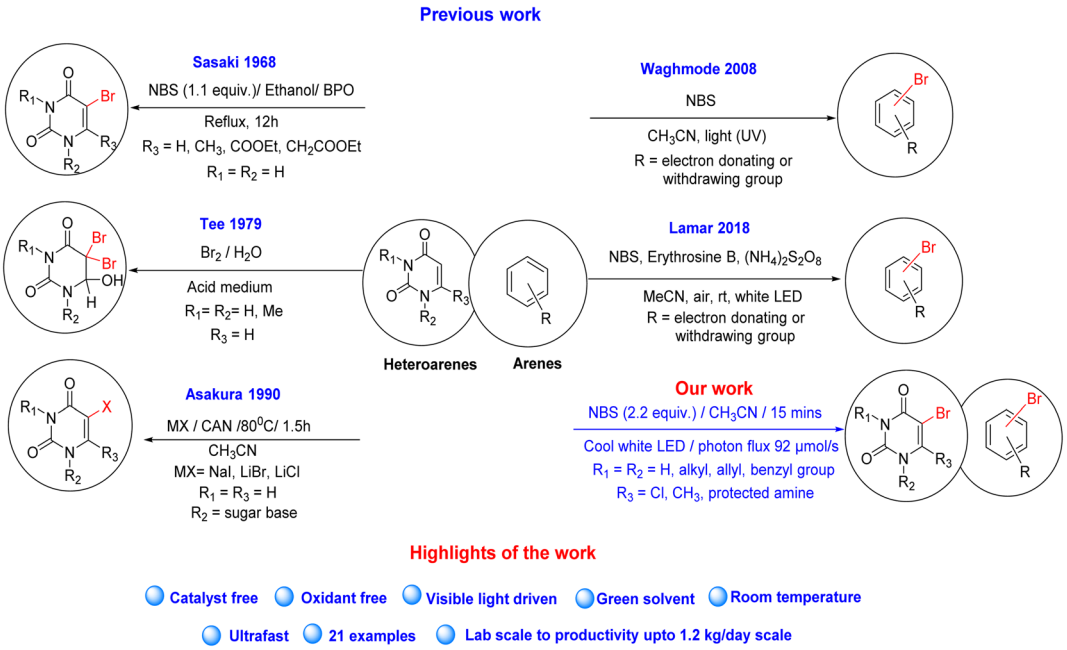

Scheme 1 Previous and our strategy for bromination of heteroarenes and arenes derivatives.

(entry 4, Table 2). So, we used 46 µmol s^{-1} photon flux as the optimum photon flux for this reaction.

Finally, we investigated the effect of solvent on this reaction. For this experiment, 1 equivalent of 6-chloro-3-methyluracil (**1**) and 2.2 equivalent of NBS were dissolved separately in 1 mL of different solvents (Table 3). A constant photon flux of 46 µmol s^{-1} was applied within the 1XA irradiation module, and the reaction was carried out with different solvents separately. In an acetonitrile solvent, product **1a** formed with a maximum yield of 84% within 1 hour (entry 1, Table 3). The product yield was very low, with a longer reaction time for other solvents (entries 2–7, Table 3). DMF also showed promising results, with almost a 79% yield in only six hours (entry 8, Table 3). This effect may be explained by the absorption spectra of the NBS in different solvents concerning the emission spectrum of the used white LEDs, which shows NBS in acetonitrile absorbs maximum in this region followed by NBS in DMF (Fig. 1 and Table S3†). Moreover, the reaction also occurred in the dark in different solvents, but the results were not so promising as compared to the light reaction (entries 9–16, Table 3). In dark conditions, both CH_3CN and DMF were relatively effective for product formation. To queue our interest, we investigated the heating effect in both solvents in the absence of light and found that the product formation was not very satisfactory after 15 hours of

Table 1 Optimization with respect to NBS[a]

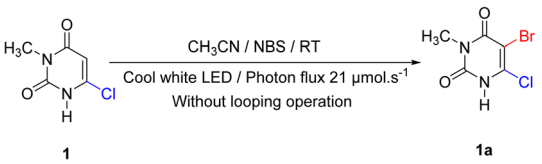

Entry	Solvent[b]	Reactant **1** (equivalent)	NBS (equivalent)	Photon flux (µmol s^{-1})	Time (h)	Yield[c] (%)
1	CH_3CN	1	1.05	21	10	48*
2	CH_3CN	1	1.3	21	10	55*
3	CH_3CN	1	1.5	21	10	67*
4	CH_3CN	1	1.8	21	10	73*
5	CH_3CN	1	2.0	21	10	77*
6	CH_3CN	1	2.2	21	5	84

[a] Reaction condition: 1 (0.6 mmol) and NBS were taken in acetonitrile. [b] Volume of solvent: 1 mL. [c] Pure product was isolated by silica-gel column chromatography, * starting material was not consumed.

Table 2 Optimization with respect to photon flux

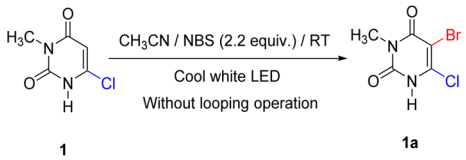

Entry	Solvent	Reactant **1** (equivalent)	NBS (equivalent)	Photon flux (μmol s^{-1})	Time (h)	Yield (%)
1	CH_3CN	1	2.2	21	5	84
2	CH_3CN	1	2.2	38	2.5	84
3	CH_3CN	1	2.2	46	1	84
4	CH_3CN	1	2.2	92	1	79

reaction (Table S2†). Hence, it can be concluded that light has a prominent role in this reaction.

With these optimal conditions, we tried to generalize the reaction with other uracil derivatives. Various *N*-substituted 6-chloro-3-methyluracil were synthesized from previously reported methods.[51] Different alkyl, allyl, and benzyl groups were found to work well with this methodology. It was found that the reactivity of the *N*-substituted alkyl and allyl groups is relatively more than that of the *N*-substituted benzyl group. Moreover, the yield of alkyl and allyl derivatives (Scheme 2, **1a**, **1e**, **1f**, **1g**, **1h**) were relatively higher than benzyl substituted derivatives (Scheme 2, **1b**, **1c**, **1d**). The reaction went well with efficient yield when other groups, such as –F and $–NO_2$, were introduced in the aryl ring.

Next, we tried to determine the scope of this methodology with other 6-substituted uracil derivatives. 6-Methyluracil was employed as the starting material, and the desired product was obtained with an efficient yield (Scheme 3, **2a**). As per our hypothesis, we tried the reaction with 6-aminouracils but failed to achieve the corresponding product. Surprisingly, when the amine group was converted to amidine by the previously reported methods,[52–55] we got the desired product with an efficient yield (Scheme 3, **2b–e**).

Next, we investigated the effectiveness of this methodology beyond uracil derivatives. 2-Aminopyrimidine, 2-amino-4-chloro-6-methylpyrimidine, and 2,4-diamino-6-chloropyrimidine were used as starting materials and

Table 3 Optimization concerning solvent[a]

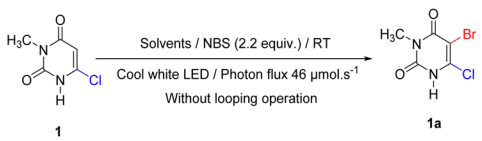

Entry	Solvent[b]b	Reagent	Cool white LED (photon flux: 46 μmol s^{-1})	Time (h)	Yield[c] (%)
1	CH_3CN	NBS	Yes	1	84
2	CH_3OH	NBS	Yes	15	45*
3	CH_3CH_2OH	NBS	Yes	15	47*
4	$CH_3COOCH_2CH_3$	NBS	Yes	15	41*
5	$CHCl_3$	NBS	Yes	15	27*
6	H_2O	NBS	Yes	15	NA
7	DMSO	NBS	Yes	15	36*
8	DMF	NBS	Yes	6	79
9	CH_3CN	NBS	Dark	15	65*
10	CH_3OH	NBS	Dark	15	33*
11	CH_3CH_2OH	NBS	Dark	15	40*
12	$CH_3COOCH_2CH_3$	NBS	Dark	15	11*
13	$CHCl_3$	NBS	Dark	15	9*
14	DMF	NBS	Dark	15	38*
15	DMSO	NBS	Dark	15	21*
16	H_2O	NBS	Dark	15	NA

[a] Reaction condition: 1 (0.6 mmol) and NBS were taken in different solvents. [b] Volume of solvent: 1 mL. [c] Pure product was isolated by silica-gel column chromatography, * starting material was not consumed.

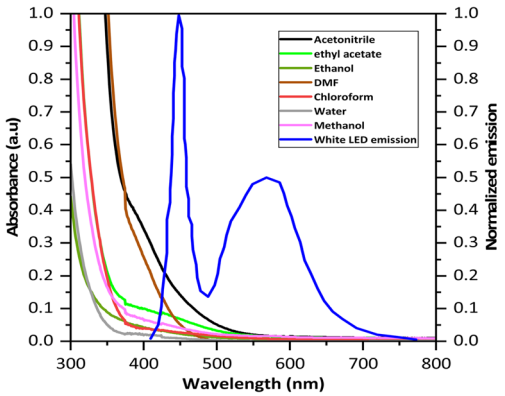

Fig. 1 Absorption spectra of NBS in different solvents at the reaction concentration and normalized emission spectra of used white LED.

obtained the desired product with good yield (Scheme 4, **3a**, **3b** and **3c**).

In addition, with this optimized condition, various brominated arene compounds were synthesized with good to excellent yields. Bromination of electron-rich aniline and phenol derivatives occurred at the *ortho* and *para* positions, including 1-naphthol and 2-naphthol, forming their corresponding dibromo products (Scheme 5). With our optimized condition, all these di and tri-substituted products were formed regioselectively.

Another exciting aspect of this reaction is that, with acetonitrile solvent, the reaction also gave a 65% yield in the absence of light in 15 hours. This phenomenon was also observed with other solvents with slow reaction rates and low yields. These findings made us curious to know the mechanistic pathway of the reaction. So, we used BHT and TEMPO as radical scavengers and carried out the same reaction in the same light source with acetonitrile as a solvent for two hours. After two hours, we found no yield with BHT and TEMPO, which was 84% in the absence of BHT and TEMPO (Fig. S6†). This implies that the reaction follows a free radical pathway.

However, free radical formation at the 6-position (sp^2 carbon) of uracil derivatives is extremely unstable. The free radical pathway was also contradicted by the fact that the same reaction also proceeded in the dark with a slow reaction rate. The requirement of 2.2 equivalents of NBS for the fast completion of the reaction in light should also have to be justified. Concerning all these facts, the possibilities of a hybrid pathway in the presence of light cannot be ignored. This means

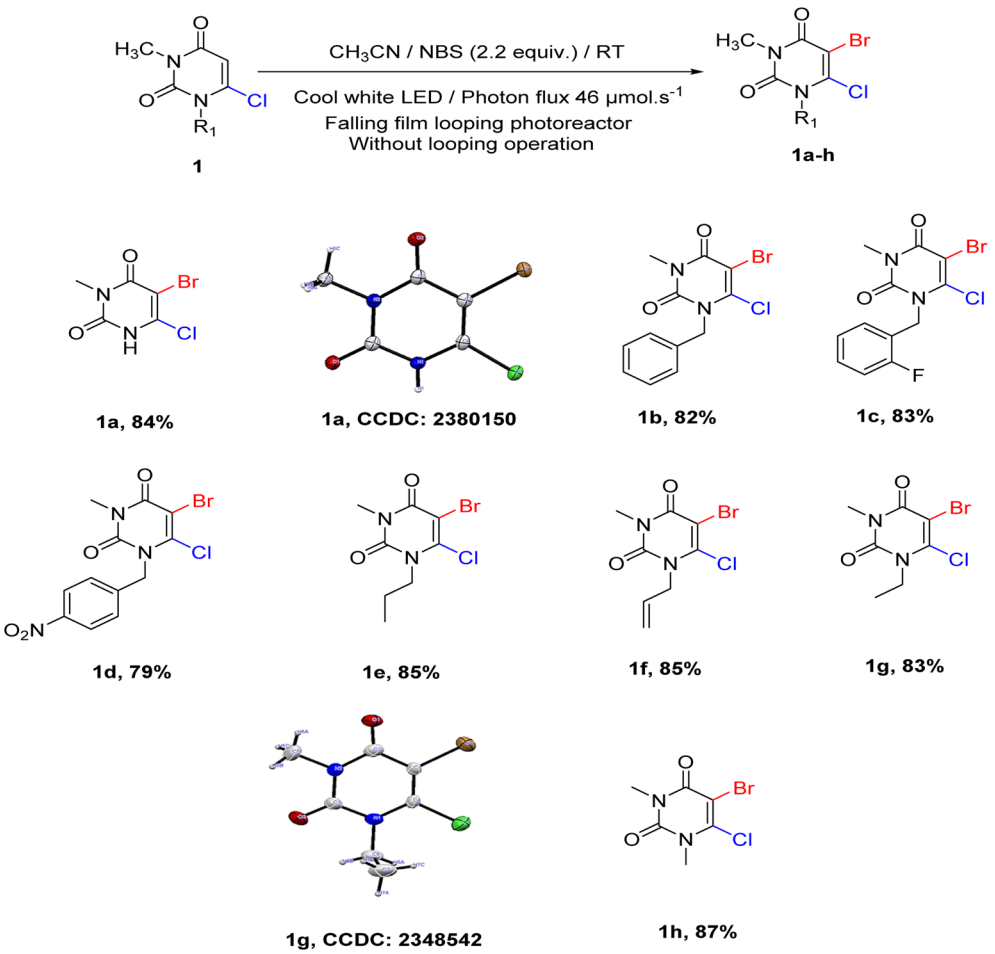

Scheme 2 Derivative scope with respect to 6-chloro-3-methyluracil.

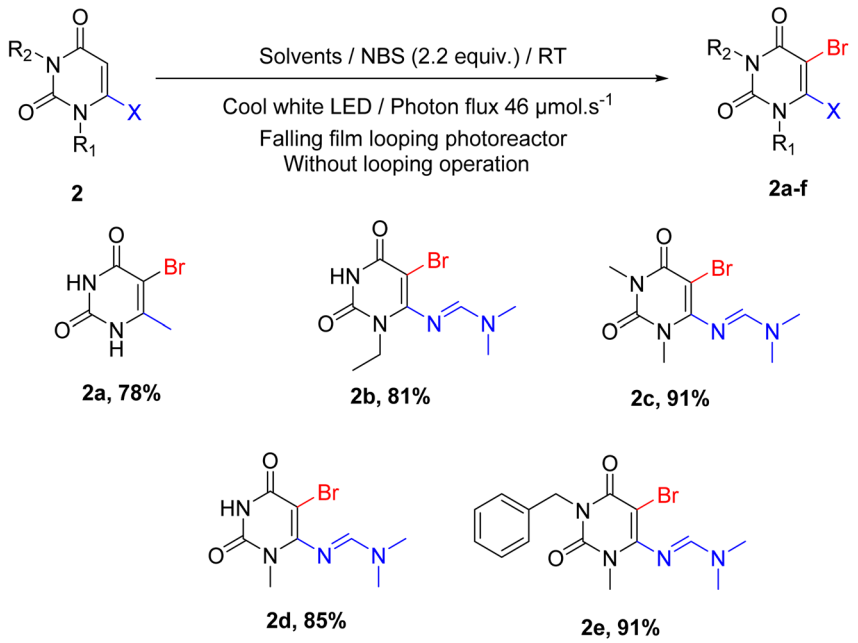

Scheme 3 Substrate scope concerning different 6-substitute, N1 and N3-substitute uracil.

first the formation of molecular bromine through the free radical pathway and then normal electrophilic substitution leading to the product. To provide sufficient evidence in favor of the proposed reaction pathway, we carried out a competitive inhibition reaction in the presence of cinnamic acid (Scheme S2†). For this, we performed the same reaction with 6-chloro-3-methyluracil and 1.5 equivalents of cinnamic acid. After two hours, no 5-brominated uracil derivative was obtained. Instead, HRMS data of the raw reaction mixture suggested the formation of 2,3-dibromo-3-phenylpropanoic acid. It proves the formation of bromine molecules during the reaction. The formation of bromine molecules can also be proved by UV-visible spectrophotometric data (Fig. 2). In this experiment, the absorbance of the reaction mixture was taken at different time intervals, and the data were compared with the absorbance data of the pure bromine molecule. It confirms the formation of bromine in the reaction mixture. The absorbance of the pure product was also taken and it did not show any peak where pure bromine peak was observed. Finally, GC-MS data of the reaction mixture confirms the formation of molecular bromine during the reaction (see details in ESI Fig. S8†). The reaction solution turns deep red during the reaction, also providing evidence in favor of the above inference.

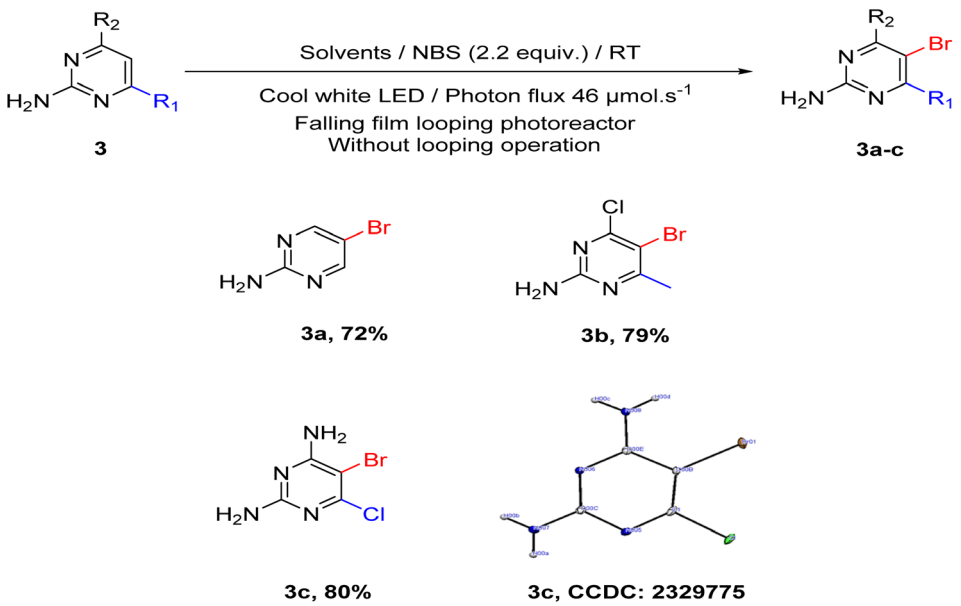

Scheme 4 Substrate scope concerning different pyrimidine derivatives.

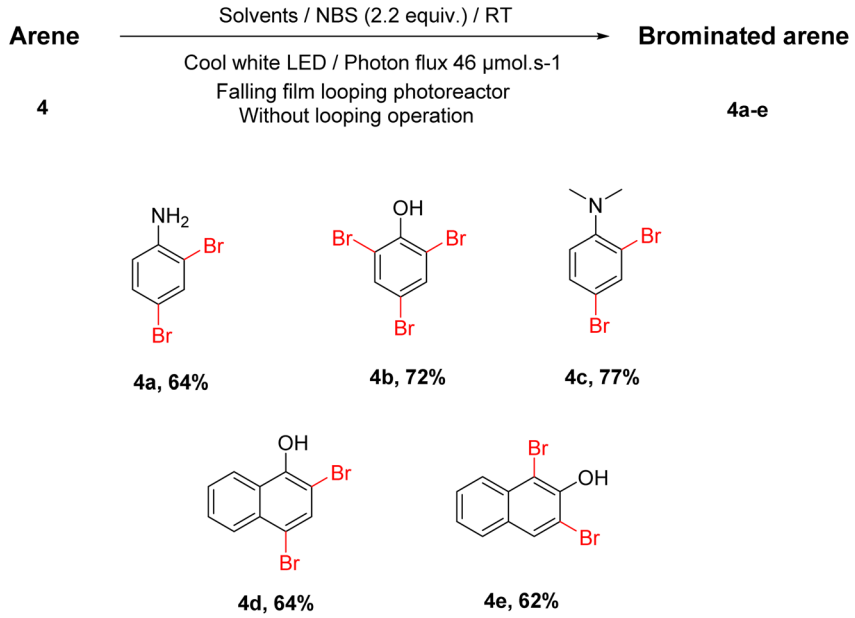

Scheme 5 Substrate scope concerning different arene derivatives.

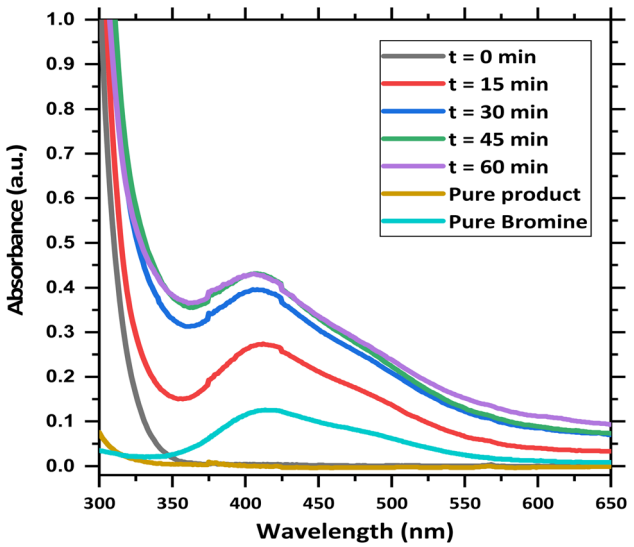

Fig. 2 Comparison of the absorbance data of the reaction mixture at different time intervals and pure product with respect to molecular bromine.

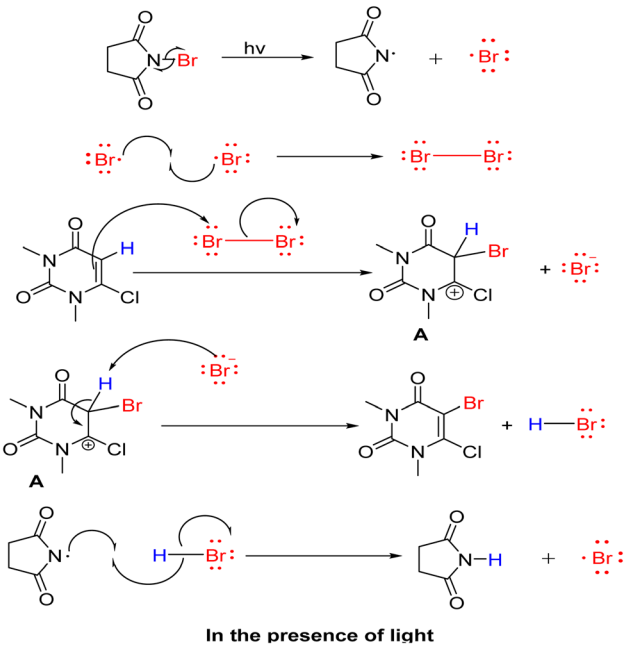

Scheme 6 Proposed reaction mechanism in the presence of light.

Based on the above experimental result, the proposed reaction mechanism is shown in Scheme 6. First, in the presence of the photons, NBS readily breaks into bromine radicals, which then combine to form molecular bromines. Secondly, the bromine molecule goes into an electrophilic substitution reaction with uracil derivatives providing intermediate **A**. Then, the deprotonation of intermediate **A** results in the formation of the desired product (Scheme 6). Bromine generation is faster in the presence of photons, so the reaction is also faster. Based on the literature, we proposed the reaction mechanism in dark conditions, and it follows a normal electrophilic substitution pathway (Scheme S1†).[56,57]

Reaction optimization with respect to different photon flux and consecutive scale-up by applying falling film looping operation

A falling film looping operation was applied for the optimization and consecutive scaling up of the reaction (see details of photoreactor in ESI Fig. S1–S4 and Table S1†). The result was analyzed by the framework for standardized reporting of data

Table 4 Optimization and scale-up strategy for the bromination of 6-chloro-3-methyluracil

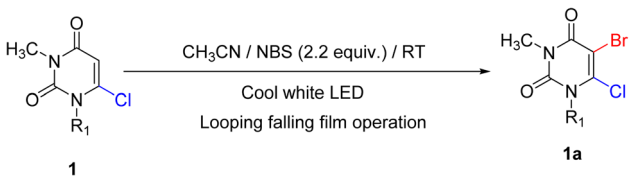

Entry	Applied photon flux (μmol s^{-1})	Space velocity (min^{-1})	Time needed (min)	Reactor module	NMR yield (%)	Separated yield (%)
1	21	15	50	1XA	89	84
2	38	15	25	1XA	89	84
3	46	15	15	1XA	84	83

for the comparative evaluation of light-driven reaction by Ziegenbalg *et al.*[58] A well-defined protocol, standardized experimental setups, and experimentally determinable performance indicators are required to provide quantitative comparability and reproducible performance evaluation across multiple systems and laboratories. In this paper, apart from synthesis and scale-up, the parameters like reactor material, reactor geometry, and dimension, positioning of the light source, the emission spectrum of the used light, used photon flux, reaction volume, operation temperature, operation mode, flow rate, absorbance data of the light absorbing species, reaction time and performance indicators like space-time yield (STE), photonic efficiency (ξ_{ext}) and reaction rate (r) are well disclosed so that reproduction of the result and comparison with other photochemical systems can be made effectively.

Optimizing different photon fluxes for the scale-up reaction was performed with a fixed falling film looping space velocity (S = 15 min^{-1}). For this, 960 mg of 6-chloro-3-methyluracil (6 mmol) was brominated by NBS (2.2 equiv.) in 10 mL acetonitrile in the 1XA reactor module and by applying different photon flux ($q_{emitted}$ = 21 μmol s^{-1}, 38 μmol s^{-1} and 46 μmol s^{-1}) separately. The corresponding time-dependent reaction monitoring was performed by thin layer chromatography (TLC) after every 5 minutes of reaction proceedings (Fig. S9†). At 21 μmol s^{-1} photon flux, the starting material was fully consumed after 50 minutes, and the corresponding NMR and separated yield were 89% and 84%, respectively (entry 1, Table 4). At 38 μmol s^{-1} photon flux, the starting material was fully consumed after 25 minutes, and the corresponding NMR and separated yield were 89% and 84%, respectively (entry 2, Table 4). This corresponds to the fact that as photon flux was almost doubled, the time required for the reaction was reduced to almost half. Similarly, at 46 μmol s^{-1} photon flux, the reactant was fully consumed after 15 minutes, and the corresponding NMR and separated yield were 84% and 83%, respectively (entry 3, Table 4). Although the photon flux increased from 21 μmol s^{-1} to 38 μmol s^{-1} and 46 μmol s^{-1} led to a decrease in the reaction time by 25 minutes and 35 minutes, respectively. Still, yield was reduced slightly at the same time, indicating product loss due to uncontrolled free radical pathway at higher photon fluxes. For this reason, we considered 46 μmol s^{-1} photon flux is optimum with the used space velocity and given looping falling film reactor parameters (Table S4 and Fig. S10–S12†).

These optimized reaction conditions for the 1XA reactor module were applied to scale up the reaction from 4.8 g-scale (30 mmol) to 9.6 g-scale (60 mmol) using 2XA and 4XA reactor modules, respectively. Sampling was done every 3 minutes, and NMR yield was calculated (Tables S5–S7 and Fig. S14–S28†). Fig. 3, left shows the result of the gradual scale-up process. It offers an almost similar trend, and the final product yield is also

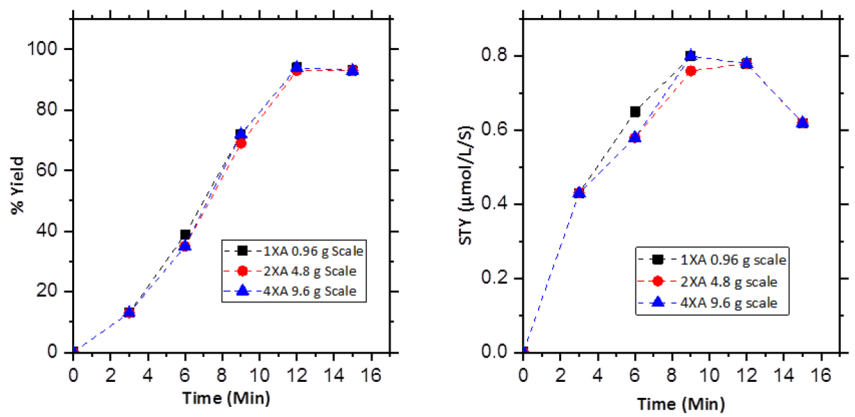

Fig. 3 Time-dependent product yield (left) and calculated STYs (right) for the successive scale process.

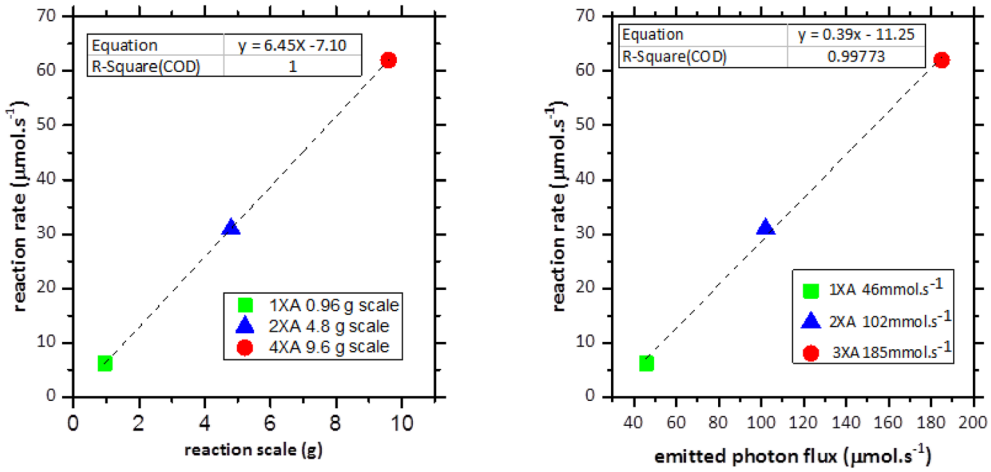

Fig. 4 Correlation graph of the reaction rate for the bromination reaction of 6-chloro-3-methyluracil with the reaction scale (left) and emitted photon flux (right) for the 1XA, 2XA and 4XA reactor modules at $\Delta t = 0$–900 s.

Table 5 Reaction rate and photonic efficiency for the bromination of 6-chloro-3-methyluracil at $\Delta t = 0$–720 s concerning different reaction modules and reaction scales

Entry	Reactor module	Reaction scale (g)	Reaction volume (mL)	Applied photon flux (μmol s^{-1})	% yield	Δt (s)	Rate (μmol s^{-1})	Photonic efficiency (ξ_{ext})
1	1XA	0.96	10	46	94	0–720	6.2	0.13
2	2XA	4.8	50	102	93	0–720	31	0.30
3	4XA	9.6	100	185	94	0–720	62	0.34

identical, indicating the effectiveness of the reactor protocol for the scaling-up approach. A very negligible drop of the STY can be observed for the 4.8 g scale and 9.6 g scale reaction in between 3 to 9 minutes of reaction time, although it becomes the same in the 12th minute of reaction proceeding (Fig. 3, right). The reaction rate ($\Delta t = 0$–720 s) also increased significantly from 6.2 μmol s^{-1} to 62 μmol s^{-1} from 0.96 g scale to 9.6 g scale. This means that the reaction rate increased 10 times with the 10 times increase of the reaction scale. For this reason, a linear increase of the reaction rate with the increasing reaction scale was observed (Fig. 4, left). This was achieved by increasing the photon flux to perfection with the increasing reaction scale and with the proper reactor design. Fig. 4 (right) shows the linear increase of the photon flux with the increasing reaction scale. The reaction rate (r) and the photonic efficiency (ξ_{ext}) also increased with the increasing reaction scale (Table 5). However, all these correlations discussed above, prove the successive scalability of the above reactions up to a 9.6 g scale per cycle with a 1.2 kg per day productivity using the falling film looping photoreactor. It also shows that the chosen scaling approach can be used for further scaling up by applying the same condition and with the scaled version of the reactor.

Conclusion

In conclusion, we have developed a novel scalable bromination method for uracil derivatives at five positions under an oxidant-free, catalyst-free, mild condition at room temperature. This method is also applicable to other pyrimidine and arene derivatives. By applying a constant photon flux of 46 μmol s^{-1} and an inexpensive reagent and solvent, a wide range of uracil, pyrimidine and arene derivatives were synthesized with good to excellent yield. Applying the falling film looping operation, the gradual scalability of the process was demonstrated, with almost maintaining the same laboratory conditions and within the same reactor with a maximum productivity of up to 1.2 kg per day. So, combined with the falling film looping photoreactor, it represents an economical, environment-friendly, and, most importantly, scalable bromination method of arene and heteroarene derivatives.

Experimental section

General procedure for small-scale reaction optimization and derivative preparation

0.6 mmol uracil derivatives and 2.2 equivalent NBS were dissolved in 1 mL solvent (acetonitrile). A constant photon flux of 46 μmol s^{-1} was applied and corresponding time-dependent reaction monitoring was performed by thin layer chromatography (TLC). After the complete consumption of the starting material, the reaction is stopped and the solvent is evaporated under reduced pressure. It was purified by column chromatography using an ethyl acetate/hexane mixture, and separated yields were measured.

Optimization for the scale-up process

In a dry 1XA reactor module, 6 mmol of 6-chloro-3-methyluracil and 2.2 equivalent of NBS (13.2 mmol) were taken, and 10 mL of

acetonitrile was added. The peristaltic pump was set with a space velocity of 15 min^{-1}. A constant photon flux of 21 μmol s^{-1} was applied, and the reaction was monitored by thin layer chromatography (TLC) until the starting material was fully consumed. After the reaction, the NMR yield and separated yield were taken (Table S4†). The same process was performed two times separately by applying 38 μmol s^{-1} and 46 μmol s^{-1} photon flux, respectively. Finally, these three reactions were monitored and the best conditions for the scale-up process were confirmed.

Gradual scale-up process by using the above optimized condition

0.96 g scale. In a dry 1XA reactor module, 6 mmol of 6-chloro-3-methyluracil and 2.2 equivalent of NBS (13.2 mmol) were taken and 10 mL of acetonitrile were added. The peristaltic pump was set with a space velocity of 15 min^{-1}. A constant photon flux of 46 μmol s^{-1} was applied for 15 minutes. The sampling was done every 3 minutes of the reaction, and NMR yields were taken (Table S5†).

4.8 g scale. In a dry 2XA reactor module, 30 mmol of 6-chloro-3-methyluracil and 2.2 equivalent of NBS (66 mmol) were taken and 50 mL of acetonitrile were added. The peristaltic pump was set with a space velocity of 15 min^{-1}. A constant photon flux of 102 μmol s^{-1} was applied for 15 minutes. The sampling was done every 3 minutes of the reaction, and NMR yields were taken (Table S6†).

9.6 g scale. In a dry 4XA reactor module, 60 mmol of 6-chloro-3-methyluracil and 2.2 equivalent of NBS (132 mmol) were taken and 100 mL of acetonitrile were added. The peristaltic pump was set with a space velocity of 15 min^{-1}. A constant photon flux of 185 μmol s^{-1} was applied for 15 minutes. The sampling was done every 3 minutes of the reaction, and NMR yields were taken (Table S7†).

Single crystal X-ray diffraction

Single crystal X-ray data for compound **1a** (CCDC: 2380150) were collected on Bruker APEX-II diffractometer with PHOTON II detector using a Mo-Kα radiation (λ = 0.71073 Å) at 293 K temperature. Data collection, refinement and reduction were performed using CrysAlisPro (ver. 1.171.42.49, 2022) program package. The crystal data and refinement parameters of compound **1a** are shown in Table S14.† Single crystal X-ray data for compound **1g** (CCDC: 2348542) were collected at 293 K temperature using a Rigaku Oxford Diffraction SuperNova diffractometer equipped with a high sensitivity EosS2 CCD detector and a Mo-Kα radiation (λ = 0.71073 Å). CrysAlisPro (ver. 1.171.40.69a, 2020) program package was used for data collection, data reduction, and absorption correction. The crystal data and refinement parameters of compound **1g** are shown in Table S15.† X-ray data for compound **3c** (CCDC: 2329775) were acquired on Bruker APEX-II diffractometer with PHOTON II detector using a Mo-Kα radiation (λ = 0.71073 Å) at 273 K temperature. Data collection and reduction were performed using APEX II and SAINT. The crystal data and refinement parameters of compound **3c** are shown in Table S16.†

Characterization data

5-Bromo-6-chloro-3-methyl pyrimidine-2,4(1*H*,3*H*)-dione (1a). White solid (120.5 mg, 84% yield), eluent: hexane/ethyl acetate (1 : 1), ^{1}H-NMR (400 MHz, DMSO-d_6) δ: 12.80 (s, 1H), 3.13 (s, 3H); ^{13}C-NMR (101 MHz, DMSO-d_6) δ: 159.33, 150.00, 143.39, 95.60, 28.63. HRMS (ESI): calculated for $C_5H_5BrClN_2O_2$ $[M + H]^+$: 238.9223; found: 238.9235.

1-Benzyl-5-bromo-6-chloro-3-methylpyrimidine-2,4(1*H*,3*H*)-dione (1b). White solid (162.4 mg, 82% yield), eluent: hexane/ethyl acetate (4 : 1), ^{1}H-NMR (400 MHz, DMSO-d_6) δ 7.36–7.25 (m, 5H), 5.29 (s, 2H), 3.25 (s, 3H). ^{13}C-NMR (101 MHz, DMSO-d_6) δ 158.18, 150.66, 145.32, 136.31, 129.07, 127.96, 127.02, 98.33, 51.67, 30.00. HRMS (ESI): calculated for $C_{12}H_{11}BrClN_2O_2$ $[M + H]^+$: 328.9692; found: 328.9684.

5-Bromo-6-chloro-1-(2-fluorobenzyl)-3-methylpyrimidine-2,4(1*H*,3*H*)-dione (1c). White solid (173.3 mg, 83% yield), eluent: hexane/ethyl acetate (4 : 1), ^{1}H-NMR (400 MHz, DMSO-d_6) δ 7.33 (dt, J = 14.4, 6.7 Hz, 2H), 7.19 (dt, J = 15.0, 9.1 Hz, 2H), 5.31 (s, 2H), 3.24 (s, 3H). ^{13}C-NMR (101 MHz, DMSO-d_6) δ 161.03, 158.21, 150.57, 145.08, 130.09, 128.55, 123.30, 115.73, 98.57, 46.17, 29.98. HRMS (ESI): calculated for $C_{12}H_{10}BrClFN_2O_2$ $[M + H]^+$: 346.9598; found: 346.9592.

5-Bromo-6-chloro-3-methyl-1-(4-nitrobenzyl)pyrimidine-2,4(1*H*,3*H*)-dione (1d). White solid (177.8 mg, 79% yield), eluent: hexane/ethyl acetate (4 : 1), ^{1}H-NMR (400 MHz, DMSO-d_6) δ: 8.17 (d, J = 8.8 Hz, 2H), 7.58 (d, J = 8.8 Hz, 2H), 5.39 (s, 2H), 3.23 (s, 3H). ^{13}C-NMR (101 MHz, DMSO-d_6) δ: 158.31, 150.67, 147.31, 145.00, 144.11, 128.14, 124.18, 98.63, 51.34, 30.02; HRMS (ESI): calculated for $C_{12}H_{10}BrClN_3O_4$ $[M + H]^+$: 373.9543; found: 373.9551.

5-Bromo-6-chloro-3-methyl-1-propylpyrimidine-2,4(1*H*,3*H*)-dione (1e). White solid (143.8 mg, 85% yield), eluent: hexane/ethyl acetate (4 : 1), ^{1}H-NMR (400 MHz, DMSO-d_6) δ: 4.01–3.95 (t, 2H), 3.20 (s, 3H), 1.61 (dt, J = 12.9, 6.5 Hz, 2H), 0.88 (t, J = 7.5 Hz, 3H); ^{13}C-NMR (101 MHz, DMSO-d_6) δ: 158.12, 150.11, 145.27, 97.68, 50.50, 29.77, 21.77, 11.17; HRMS (ESI): calculated for $C_8H_{11}BrClN_2O_2$ $[M + H]^+$: 280.9692; found: 280.9686.

1-Allyl-5-bromo-6-chloro-3-methylpyrimidine-2,4(1*H*,3*H*)-dione (1f). White solid (142.8 mg, 85% yield), eluent: hexane/ethyl acetate (4 : 1), ^{1}H-NMR (500 MHz, DMSO-d_6) δ: 4.68–4.61 (m), 4.49 (t, J = 7.0 Hz), 4.04 (dd, J = 11.1, 5.8 Hz), 3.93 (dd, J = 11.1, 5.8 Hz), 3.19 (s); ^{13}C-NMR (126 MHz, DMSO-d_6) δ: 158.09, 150.33, 145.07, 98.62, 53.15, 50.16, 36.46, 29.92; HRMS (ESI): calculated for $C_8H_9BrClN_2O_2$ $[M + H]^+$: 278.9536; found: 278.9532.

5-Bromo-6-chloro-1-ethyl-3-methylpyrimidine-2,4(1*H*,3*H*)-dione (1g). White solid (133.5 mg, 83% yield), eluent: hexane/ethyl acetate (4 : 1), ^{1}H-NMR (500 MHz, DMSO-d_6) δ: 4.06 (q, J = 7.1 Hz, 2H), 3.18 (s, 3H), 1.17 (t, J = 7.1 Hz, 3H); ^{13}C-NMR (126 MHz, DMSO-d_6) δ: 158.19, 149.98, 145.20, 97.66, 44.66, 29.78, 13.93; HRMS (ESI): calculated for $C_7H_9BrClN_2O_2$ $[M + H]^+$: 266.9536; found: 266.9538.

5-Bromo-6-chloro-1,3-dimethylpyrimidine-2,4(1*H*,3*H*)-dione (1h). White solid (132.1 mg, 87% yield), eluent: hexane/ethyl acetate (3.5 : 1.5), ^{1}H-NMR (500 MHz, DMSO-d_6) δ: 3.18 (s, 3H), 3.18 (s, 3H); ^{13}C-NMR (126 MHz, DMSO-d_6) δ: 163.37,

163.11, 150.10, 60.42, 30.45, 30.31; HRMS (ESI): calculated for $C_6H_7BrClN_2O_2$ $[M + H]^+$: 252.9379; found: 252.9371.

5-Bromo-6-methylpyrimidine-2,4(1*H*,3*H*)-dione (2a). White solid (95.9 mg, 78% yield), eluent: hexane/ethyl acetate (7 : 3), ^{1}H-NMR (400 MHz, DMSO-d_6) δ: 11.38 (s, 1H), 11.25 (s, 1H), 2.19 (s, 3H); ^{13}C-NMR (101 MHz, DMSO-d_6) δ: 160.43, 151.81, 150.68, 95.44, 19.93. HRMS (ESI): calculated for $C_5H_5BrN_2NaO_2$ $[M + Na]^+$: 226.9432; found: 226.9517.

(*E*)-*N*′-(5-Bromo-3-ethyl-2,6-dioxo-1,2,3,6-tetrahydropyrimidin-4-yl)-*N*,*N*-dimethylformimidamide (2b). Brown, solid (140.5 mg, 81% yield), eluent: 100% ethyl acetate ^{1}H-NMR (500 MHz, DMSO-d_6) δ: 11.44 (s, 1H), 8.64 (s, 1H), 3.60 (dd, J = 13.9, 7.1 Hz, 2H), 3.21 (s, 6H), 1.06 (t, J = 7.2 Hz, 3H); ^{13}C-NMR (126 MHz, DMSO-d_6) δ: 160.02, 155.35, 150.23, 136.58, 86.92, 30.04, 14.28; HRMS (ESI): calculated for $C_9H_{14}BrN_4O_2$ $[M + H]^+$: 289.0300; found: 289.0313.

(*E*)-*N*′-(5-Bromo-1,3-dimethyl-2,6-dioxo-1,2,3,6-tetrahydropyrimidin-4-yl)-*N*,*N*-dimethylformimidamide (2c). Reddish brown, solid (157.8 mg, 91% yield), eluent: 100% ethyl acetate, ^{1}H-NMR (400 MHz, DMSO-d_6) δ: 7.93 (s, 1H), 3.26 (s, 3H), 3.20 (s, 3H), 3.11 (s, 3H), 3.00 (s, 3H); ^{13}C-NMR (101 MHz, DMSO-d_6) δ: 159.51, 157.59, 157.13, 151.15, 82.39, 40.56, 34.47, 31.87, 29.19; HRMS (ESI): calculated for $C_9H_{14}BrN_4O_2$ $[M + H]^+$: 289.0300; found: 289.0308.

(*E*)-*N*′-(5-Bromo-3-methyl-2,6-dioxo-1,2,3,6-tetrahydropyrimidin-4-yl)-*N*,*N*-dimethylformimidamide (2d). Darkish brown, solid (140.2 mg, 85% yield), eluent: 100% ethyl acetate ^{1}H-NMR (400 MHz, DMSO-d_6) δ: 11.25 (s, 1H), 7.93 (s, 1H), 3.18 (s, 3H), 3.10 (s, 3H), 2.99 (s, 3H); ^{13}C-NMR (101 MHz, DMSO-d_6) δ: 160.00, 158.53, 157.55, 150.85, 82.68, 40.53, 34.45, 30.87; HRMS (ESI): calculated for $C_8H_{12}BrN_4O_2$ $[M + H]^+$: 275.0144; found: 275.0137.

(*E*)-*N*′-(1-Benzyl-5-bromo-3-methyl-2,6-dioxo-1,2,3,6-tetrahydropyrimidin-4-yl)-*N*,*N*-dimethylformimidamide (2e). Pale yellow, solid (199.3 mg, 91% yield), eluent: hexane/ethyl acetate (1 : 1), ^{1}H-NMR (400 MHz, DMSO-d_6) δ 7.89 (s, 1H), 7.29–7.18 (m, 5H), 4.98 (s, 2H), 3.23 (s, 3H), 3.05 (s, 3H), 2.96 (s, 3H); ^{13}C-NMR (101 MHz, DMSO-d_6) δ 163.06, 159.42, 157.60, 151.13, 137.77, 128.75, 127.96, 127.61, 82.39, 45.23, 34.47, 31.96, 29.92; HRMS (ESI): calculated for $C_{15}H_{18}BrN_4O_2$ $[M + H]^+$: 365.0613; found: 365.0615.

5-Bromopyrimidin-2-amine (3a). Light pink, solid (75.2 mg, 72% yield), eluent: hexane/ethyl acetate (1 : 1), ^{1}H-NMR (400 MHz, DMSO-d_6) δ: 8.30 (s, 2H), 6.86 (s, 2H); ^{13}C-NMR (101 MHz, DMSO-d_6) δ: 162.42, 158.55, 105.62; HRMS (ESI): calculated for $C_4H_5BrN_3$ $[M + H]^+$: 173.9667; found: 173.9673, spectroscopic data matched with ref. 59.

5-Bromo-4-chloro-6-methylpyrimidin-2-amine (3b). White solid (105.2 mg, 79% yield), eluent: hexane/ethyl acetate (3 : 2), ^{1}H-NMR (400 MHz, DMSO-d_6) δ 6.77 (s, 2H), 2.33 (s, 3H); ^{13}C-NMR (101 MHz, DMSO-d_6) δ 169.51, 161.11, 159.59, 104.52, 25.44; HRMS (ESI): calculated for $C_5H_6BrClN_3$ $[M + H]^+$: 221.9434; found: 221.9425.

5-Bromo-6-chloropyrimidine-2,4-diamine (3c). White solid (107 mg, 80% yield), eluent: hexane/ethyl acetate (1 : 1), ^{1}H-NMR (400 MHz, DMSO-d_6) δ: 7.02 (s, 1H), 6.53 (s, 1H); ^{13}C-NMR (101 MHz, DMSO-d_6) δ: 162.46, 161.50, 157.63, 86.74; HRMS (ESI): calculated for $C_5H_5BrClN_4$ $[M + H]^+$: 222.9386; found: 222.9391.

2,4-Dibromoaniline (4a). Yield: 96.4 mg, 64%; ^{1}H-NMR (400 MHz, $CDCl_3$) δ 7.52 (s, 1H), 7.19 (d, J = 8.5 Hz, 1H), 6.62 (d, J = 8.5 Hz, 1H), 4.06 (s, 2H); ^{13}C-NMR (101 MHz, $CDCl_3$) δ 143.28, 134.46, 131.19, 116.76, 109.61. Spectroscopic data matched with ref. 60.

2,4,6-Tribromophenol (4b). Yield: 142.9 mg, 72%; ^{1}H-NMR (400 MHz, $CDCl_3$) δ 7.59 (s, 2H), 5.87 (s, 1H); ^{13}C-NMR (101 MHz, $CDCl_3$) δ 148.95, 134.24, 112.72, 110.42. Spectroscopic data matched with ref. 61.

2,4-Dibromo-*N*,*N*-dimethylaniline (4c). Yield: 128.9 mg, 77%; ^{1}H-NMR (400 MHz, $CDCl_3$) δ 7.68 (s, 1H), 7.36 (d, J = 10.9 Hz, 1H), 6.94 (d, J = 8.6 Hz, 1H), 2.78 (s, 6H); ^{13}C-NMR (101 MHz, $CDCl_3$) δ 151.15, 136.04, 131.01, 121.64, 119.69, 115.36, 44.11. Spectroscopic data matched with ref. 62.

2,4-Dibromonaphthalen-1-ol (4d). Yield: 115.9 mg, 64%; (400 MHz, $CDCl_3$) δ 8.25 (d, J = 8.4 Hz, 1H), 8.13 (d, J = 8.3 Hz, 1H), 7.79 (s, 1H), 7.63 (t, J = 7.0 Hz, 1H), 7.56 (t, J = 7.5 Hz, 1H), 5.97 (s, 1H); ^{13}C-NMR (101 MHz, $CDCl_3$) δ 148.18, 131.89, 131.11, 128.17, 127.15, 126.95, 125.09, 122.81, 113.35, 103.20.

1,3-Dibromonaphthalen-2-ol (4e). Yield: 112.3 mg, 62%; ^{1}H-NMR (400 MHz, $CDCl_3$) δ 7.90 (dd, J = 16.5, 5.4 Hz, 2H), 7.61 (dd, J = 12.6, 5.5 Hz, 2H), 7.27 (s, 1H), 5.93 (s, 1H); ^{13}C-NMR (101 MHz, $CDCl_3$) δ 150.91, 131.05, 130.61, 130.09, 128.40, 127.23, 118.29, 106.13.

Data availability

The data supporting this article have been included as part of the main article and ESI.† Crystallographic data for compound **1a** (CCDC = 2380150), **1g** (CCDC = 2348542) and **3c** (CCDC = 2329775) have been deposited at the CCDC.

Author contributions

S. Naskar and S. Mal have contributed equally towards conceptualization, investigation, data curation, validation, visualization, writing of the manuscript and ESI.† S. Shivangi supported it with experimentation, data curation, formal analysis, and analytical results. S. Das contributed towards conceptualization, investigation, resources, funding acquisition, overall supervision, writing and review of the manuscript and ESI.†

Conflicts of interest

There are no conflicts to declare.

Acknowledgements

We thank NIT Patna for providing the research facility and DST grant (EEQ/2019/000294) and BRNS project (54/14/15/2020-BRNS/35054) for financial assistance. We also thank Dr Chris Hebert for his kind help to solve the crystal structure. We would like to thank Dr Rima Thakur for her vital opinions regarding

this work. We would like to thank IIT(ISM) Dhanbad and SAIF IIT Patna for their instrumental facilities.

References

1 P. L. Stetson, D. P. Normolle, J. A. Knol, J. Norma, Z. Yang, E. Sakmar, D. Prieskorn, P. Terrio, C. A. Knutsen and W. D. Ensminger, *J. Natl. Cancer Inst.*, 1991, **83**, 2532–2540.
2 D. Ramesh, B. G. Vijayakumar and T. Kannan, *Eur. J. Med. Chem.*, 2020, **207**, 112801.
3 M. N. Lone, S. Gul, U. Mehraj, S. Sofi, A. H. Dar, S. A. Ganie, N. A. Wani, M. A. Mir and M. A. Zargar, *Appl. Biochem. Biotechnol.*, 2023, **195**, 6212–6231.
4 A. V. Aerschot, D. Everaert, J. Balzarini, K. Augustyns, L. Jie, G. Janssen, O. Peeters, N. Blaton and C. D. Ranter, *J. Med. Chem.*, 1990, **33**, 1833–1839.
5 A. Pa and D. Cie, *Eur. J. Med. Chem.*, 2015, **97**, 582–611.
6 S. Mal and S. Das, *ChemistrySelect*, 2023, **8**, e202302146.
7 J. R. Mercer, L. H. Xu, E. E. Knaus and L. I. Wiebe, *J. Med. Chem.*, 1989, **32**, 1289–1294.
8 Y. Kobayashi, K. Yamamoto, T. Asai, M. Nakano and I. Kumadaki, *J. Chem. Soc. Chem. Commun.*, 1980, 2755–2761.
9 Y. Choi, L. Li, S. Grill, E. Gullen, C. S. Lee, G. Gumina, E. Tsujii, Y. C. Cheng and C. K. Chu, *J. Med. Chem.*, 2000, **43**, 2538–2546.
10 B. Loddo, S. Muntoni and W. Ferrari, *Nature*, 1963, **198**, 510.
11 K. Felczak, A. Miazga, J. Poznański, M. Bretner, T. Kulikowski, J. M. Dzik, B. Golos, Z. Zielinski, J. Ciesla and W. Rode, *J. Med. Chem.*, 2000, **43**, 4647–4656.
12 Y. B. Platonova, A. N. Volov and L. G. Tomilova, *Bioorg. Med. Chem. Lett.*, 2020, **30**, 127351.
13 T. Akiyama, F. Simeno, M. Murakami and F. Yoneda, *J. Am. Chem. Soc.*, 1992, **114**, 6613–6620.
14 V. Srivastava, P. K. Singh, A. Srivastava and P. P. Singh, *RSC Adv.*, 2021, **11**, 14251–14259.
15 R. Nencka, I. Votruba, H. Hřebabecký, E. Tloušťová, K. Horská, M. Masojídková and A. Holý, *Bioorg. Med. Chem. Lett.*, 2006, **16**, 1335–1337.
16 X. L. Li, W. Wu, X. H. Fan and L. M. Yang, *RSC Adv.*, 2013, **3**, 12091–12095.
17 R. Semwal, C. Ravi, R. Kumar, R. Meena and S. Adimurthy, *J. Org. Chem.*, 2019, **84**, 792–805.
18 T. Xu, W. Zhou, J. Wang, X. Li, J. W. Guo and B. Wang, *Tetrahedron Lett.*, 2014, **55**, 5058–5061.
19 J. Berthelot, C. Guette, P. L. Desbène, J. J. Basselier, P. Chaquin and D. Masure, *Can. J. Chem.*, 1989, **67**, 2061–2066.
20 Y. Wu, S. Xu, H. Wang, D. Shao, Q. Qi, Y. Lu, L. Ma, J. Zhou, W. Hu, W. Gao and J. Chen, *J. Org. Chem.*, 2021, **86**, 16144–16150.
21 O. S. Tee and C. G. Berks, *J. Org. Chem.*, 1980, **45**, 830–835.
22 O. S. Tee and S. Banerjee, *Can. J. Chem.*, 1979, **57**, 626–634.
23 S. Banerjee and O. S. Tee, *J. Org. Chem.*, 1974, **39**, 3120–3125.
24 H. Ren, Y. Yang, J. Lin, Y. Qi and Y. Zhang, *Front. Chem. China*, 2008, **3**, 152–156.
25 H. Veisi, R. Ghorbani-Vaghei and M. A. Zolfigol, *Org. Prep. Proced. Int.*, 2011, **43**, 489–540.
26 C. Djerassi, *Chem. Rev.*, 1948, **43**, 271–317.
27 T. Sasaki and M. Ando, *Bull. Chem. Soc. Jpn.*, 1968, **41**, 2215–2217.
28 R. O. Recknagel, E. A. Glende, J. A. Dolak and R. L. Waller, *Pharmacol. Ther.*, 1989, **43**, 139–154.
29 A. S. Rood, P. D. McGavran, J. W. Aanenson and J. E. Till, *Risk Anal.*, 2001, **21**, 675–695.
30 United Nations Environment Programme, Ozone Secretariat, *The Montreal Protocol on Substances that Deplete the Ozone Layer as Either Adjusted and/or Amended in London 1990, Copenhagen 1992, Vienna 1995, Montreal 1997, and Beijing 1999*, United Nations Environment Programme, Nairobi, Kenya, 2000.
31 Y. Liu, B. Zhang, D. Yan and X. Xiang, *Green Chem.*, 2024, **26**, 2505–2524.
32 P. Li, T. Zhang, M. A. Mushtaq, S. Wu, X. Xiang and D. Yan, *Chem. Rec.*, 2021, **21**, 841–857.
33 L. Yao, D. Wei, Y. Ni, D. Yan and C. Hu, *Nano Energy*, 2016, **26**, 248–256.
34 D. Shao, Y. Wu, S. Hu, W. Gao, Y. Du, X. Jia and J. Chen, *ACS Sustain. Chem. Eng.*, 2022, **10**, 10294–10302.
35 C. H. M. Amijs, G. P. M. Van Klink and G. Van Koten, *Green Chem.*, 2003, **5**, 470–474.
36 R. Mestres and J. Palenzuela, *Green Chem.*, 2002, **4**, 314–316.
37 A. Podgoršek, S. Stavber, M. Zupan and J. Iskra, *Tetrahedron Lett.*, 2006, **47**, 1097–1099.
38 A. Podgoršek, S. Stavber, M. Zupan and J. Iskra, *Tetrahedron Lett.*, 2006, **47**, 7245–7247.
39 M. Jereb, M. Zupan and S. Stavber, *Helv. Chim. Acta*, 2009, **92**, 555–566.
40 H. Shaw, H. D. Perlmutter, C. Gu, S. D. Arco and T. O. Quibuyen, *J. Org. Chem.*, 1997, **62**, 236–237.
41 P. K. Chhattise, A. V. Ramaswamy and S. B. Waghmode, *Tetrahedron Lett.*, 2008, **49**, 189–194.
42 D. A. Rogers, R. G. Brown, Z. C. Brandeburg, E. Y. Ko, M. D. Hopkins, G. LeBlanc and A. A. Lamar, *ACS Omega*, 2018, **3**, 12868–12877.
43 P. Li, Y. Liu, M. A. Mushtaq and D. Yan, *Inorg. Chem. Front.*, 2023, **10**, 4650–4667.
44 X. Fang, R. Gao, Y. Yang and D. Yan, *Iscience*, 2019, **16**, 22–30.
45 X. Fang, Y. Tang, Y. J. Ma, G. Xiao, P. Li and D. Yan, *Sci. China Mater.*, 2023, **66**, 664–671.
46 V. Srivastava, P. K. Singh and P. P. Singh, *J. Photochem. Photobiol., C*, 2022, **50**, 100488.
47 J. W. Beatty, J. J. Douglas, K. P. Cole and C. R. Stephenson, *Nat. Commun.*, 2015, **6**, 7919.
48 D. Cantillo, O. De Frutos, J. A. Rincon, C. Mateos, C. Oliver Kappe and E. F. Schroeder, *J. Org. Chem.*, 2014, **79**, 223–229.
49 S. Naskar, D. Kowalczyk, S. Mal, S. Das, D. Mandal, P. Kumar and D. Ziegenbalg, *React. Chem. Eng.*, 2023, **8**, 2211–2222.
50 S. Naskar, S. Mal, S. Shivangi and S. Das, *ChemRxiv*, 2023, preprint, DOI: **10.26434/chemrxiv-2023-7s2nm**.
51 P. Debnath, G. Sahu and U. C. De, *ChemistrySelect*, 2019, **4**, 2327–2332.
52 K. Dzieszkowski, I. Barańska and Z. Rafiński, *J. Org. Chem.*, 2020, **85**, 6645–6662.

53 V. Papesch and E. F. Schroeder, *J. Org. Chem.*, 1951, **16**, 1879–1890.
54 A. J. Thakur, S. Das and A. K. Phukan, *J. Mol. Struct.*, 2009, **929**, 134–140.
55 N. S. Freeman, C. E. Moore, L. M. Wilhelmsson and Y. Tor, *J. Org. Chem.*, 2016, **81**, 4530–4539.
56 W. Lorpaiboon and P. Bovonsombat, *Org. Biomol. Chem.*, 2021, **19**, 7518–7534.
57 M. C. Carreño, J. G. Ruano, G. Sanz, M. A. Toledo and A. Urbano, *Tetrahedron Lett.*, 1996, **37**, 4081–4084.
58 D. Ziegenbalg, A. Pannwitz, S. Rau, B. Dietzek-Ivanšić and C. Streb, *Angew. Chem., Int. Ed. Engl.*, 2022, **61**, e202114106.
59 M. B. Smith, L. Guo, S. Okeyo, J. Stenzel, J. Yanella and E. LaChapelle, *Org. Lett.*, 2002, **4**, 2321–2323.
60 J. M. Chrétien, F. Zammattio, E. Le Grognec, M. Paris, B. Cahingt, G. Montavon and J. P. Quintard, *J. Org. Chem.*, 2005, **70**, 2870–2873.
61 S. Adimurthy, G. Ramachandraiah, A. V. Bedekar, S. Ghosh, B. C. Ranu and P. K. Ghosh, *Green Chem.*, 2006, **8**, 916–922.
62 M. P. Doyle, M. A. Van Lente, R. Mowat and W. F. Fobare, *J. Org. Chem.*, 1980, **45**, 2570–2575.